

Distribution of calcium phosphate in the exoskeleton of larval *Exeretonevra angustifrons* Hardy (Diptera: Xylophagidae)

Bronwen W. Cribb^{a,b,*}, Ron Rasch^a, John Barry^a, Christopher M. Palmer^{b,1}

^aCentre for Microscopy and Microanalysis, The University of Queensland, Brisbane, Qd 4072, Australia

^bDepartment of Zoology and Entomology, The University of Queensland, Brisbane, Qd 4072, Australia

Received 28 July 2004; accepted 26 August 2004

Abstract

Distribution and organisation of the mineral, amorphous calcium phosphate (ACP), has been investigated in the exoskeleton of the xylophagid fly larva *Exeretonevra angustifrons* Hardy. While head capsule and anal plate are smooth with a thin epicuticle, the epicuticle of the body is thicker and shows unusual micro-architecture comprised of minute hemispherical (dome-shaped) protrusions. Electron microprobe analysis and energy dispersive spectroscopy revealed heterogeneity of mineral elements across body cuticle and a concentration of ACP in the epicuticle, especially associated with the hemispherical structures. Further imaging and analysis showed the bulk of the ACP to be present in nano-sized granules. It is hypothesised that the specific distribution of ACP may enhance cuticular hardness or durability without reducing flexibility.

© 2004 Elsevier Ltd. All rights reserved.

Keywords: Insect; Cuticle; Integument; Hardening; Analytical electron microscopy; Electron microprobe

1. Introduction

Strengthening of biological structures through cuticular calcification is well developed in decapod crustaceans but it rarely occurs in insects, where it is poorly understood (Fraenkel and Hsiao, 1967; Gilby and McKellar, 1976; Roseland et al., 1985). Grodowitz and Broce (1983) attempted quantification of calcification in insects at the bulk scale. However, more recently we have quantified the calcium mineral content in the cuticle of a larval insect, *Exeretonevra angustifrons* Hardy, at the micron scale (Rasch et al., 2003). That study on the putatively predatory maggot investigated elemental composition and measured the concentration of calcium and phosphorus, showing that the inorganic component was present at high levels in a ratio concomitant with amorphous calcium phosphate (ACP) and

was distributed heterogeneously. Further investigation of the distribution of the mineral phase at the micron and nanometre level is needed to discover where deposition is occurring and how this might affect exoskeletal organisation. This is the focus of the current study.

2. Materials and methods

First instar larvae of the fly, *Exeretonevra angustifrons* were reared from eggs and prepared for analysis in a number of ways.

2.1. Scanning electron microscopy

Samples for scanning electron microscopy (SEM) were preserved in 80% ethanol, dehydrated to 100% ethanol, infiltrated with hexamethyldisilazane and air-dried before being mounted on an aluminium stub with double-sided adhesive and coated with carbon via evaporation in vacuum. For gross identification of calcium rich regions, samples

* Corresponding author. Centre for Microscopy and Microanalysis, The University of Queensland, Brisbane, Qd 4072, Australia. Tel.: +61 7 3365 7086; fax: +61 7 3365 2199.

E-mail address: b.cribb@uq.edu.au (B.W. Cribb).

¹ Present address: School of Botany and Zoology, The Australian National University, Canberra ACT 0200, Australia.

were imaged using primary and secondary electron signals in JEOL JSM-6300F and Philips XL30 SEMs at 20 kV.

2.2. Transmission electron microscopy

Five head capsule, body and anal plate samples were preserved in 80% ethanol, dehydrated to 100% ethanol, embedded in Spurr resin and polymerised at 60 °C for 3 days. Tissue was then sectioned using a diamond knife and stained with uranyl acetate and Reynold's lead citrate before mounting on copper grids for viewing. Images of ultra-structure were obtained using a JEOL 1010 transmission electron microscope (TEM) at 80 kV.

2.3. Analytical electron microscopy

Tissue sections for analytical electron microscopy (AEM) were obtained from material prepared and sectioned under the TEM protocol above, except that tissue was left unstained. To evaluate composition of targeted cuticular regions as well as adjacent tissue and resin regions (controls), energy dispersive spectroscopy was used (Oxford Si (Li) ATW detector model 6498 attached to a JEOL 2010 AEM used in spot and area mode). A JEOL 2010 AEM was also used in electron diffraction mode to assess the crystalline nature of regions evaluated for composition.

2.4. Electron microprobe analysis

The head capsule, body and anal plate of two larvae used to obtain sections for TEM were re-embedded in resin to provide a larger surface and polished down to the tissue cross section using silicon carbide paper and diamond paste (minimum 0.25 µm), rinsing in ethanol between stages. The specimens were then ultrasonically cleaned in ethanol and carbon coated with 20 nm of carbon in a JEOL JEE-4X vacuum evaporator. Elemental maps of the tissue cross section were produced using a JEOL JXA-8800L microprobe with four wavelength dispersive X-ray spectrometers (WDS). Four elements were mapped for X-ray intensity in parallel: P, Ca, S and N. The X-ray peaks were determined on the analytical standards (supplied by Charles M. Taylor Co., Stanford California, USA) and diffracting crystals in Table 1. The microprobe was operated at 15 kV accelerating voltage, with a 30 nA beam current and a probe diameter of 2 µm (defocused to reduce specimen damage). A suitable

area was mapped with a 100×100 pixel scan, a 2 µm step size, and a 4 s dwell time, for a 12 h and 16 min X-ray intensity map.

3. Results

3.1. Scanning electron microscopy

The larva appears maggot-like with a pointed head capsule (Fig. 1A). Numerous dome-shaped or hemispherical protuberances are seen on the body (Fig. 1B), which differs from the smooth head and anal plate (Fig. 1C). In backscatter mode, which discriminates between atomic weight, these hemispheres are seen as differing in intensity and therefore composition, from the rest of the cuticle. They are composed of a heavier element or elements (Fig. 1D and E). The hemispheres range from 0.5–5 µm in diameter and average 59/50 µm² for those of 1 µm and larger.

3.2. Transmission electron microscopy

In transverse section the cuticle of both head capsule and anal plate show a flat surface and in cross section the cuticle appears homogeneous, grading into an electron-dense epicuticle, 0.5 µm in thickness (Fig. 2A and B). The cuticle was observed to vary in thickness from 2 to 22 µm (not shown). In contrast the body cuticle is no greater than 12 µm at its maximum thickness and has a thicker inner epicuticle consisting of a ragged electron-dense base, 0.7–4 µm thick (Fig. 2C). This layer is penetrated by numerous pore canals (Fig. 2D). Overlying it is a less electron-dense outer epicuticle of 0.7–4 µm thickness, in which electron-dense clumps of material (Fig. 2C and D) or hemispheres (Fig. 2E and F) are visible, producing a rough surface. When hemispheres are present they are ventrally bounded by a fine electron-dense line (Fig. 2F). A crust of putative waxes and/or cements is sometimes seen overlying this layer (Fig. 2E).

3.3. Analytical electron microscopy

Tissue viewed in unstained form showed differences in contrast related to composition. Electron-dense granules are seen around and within the hemispherical protuberances (Fig. 3) and are also seen in the electron-dense line on which these domes sit (Fig. 3). The arrangement of ACP in the epicuticle is shown diagrammatically in Fig. 4. The granules

Table 1
Standards and diffracting crystals used for electron microprobe analysis

Element	X-ray	Standard	Crystal	2D spacing (nm)
Ca	K α	Apatite	PET	0.8742
P	K α	Apatite	TAP	2.5757
S	K α	FeS ₂	PET	0.8742
N	K α	BN	LDE1	5.8–6.2

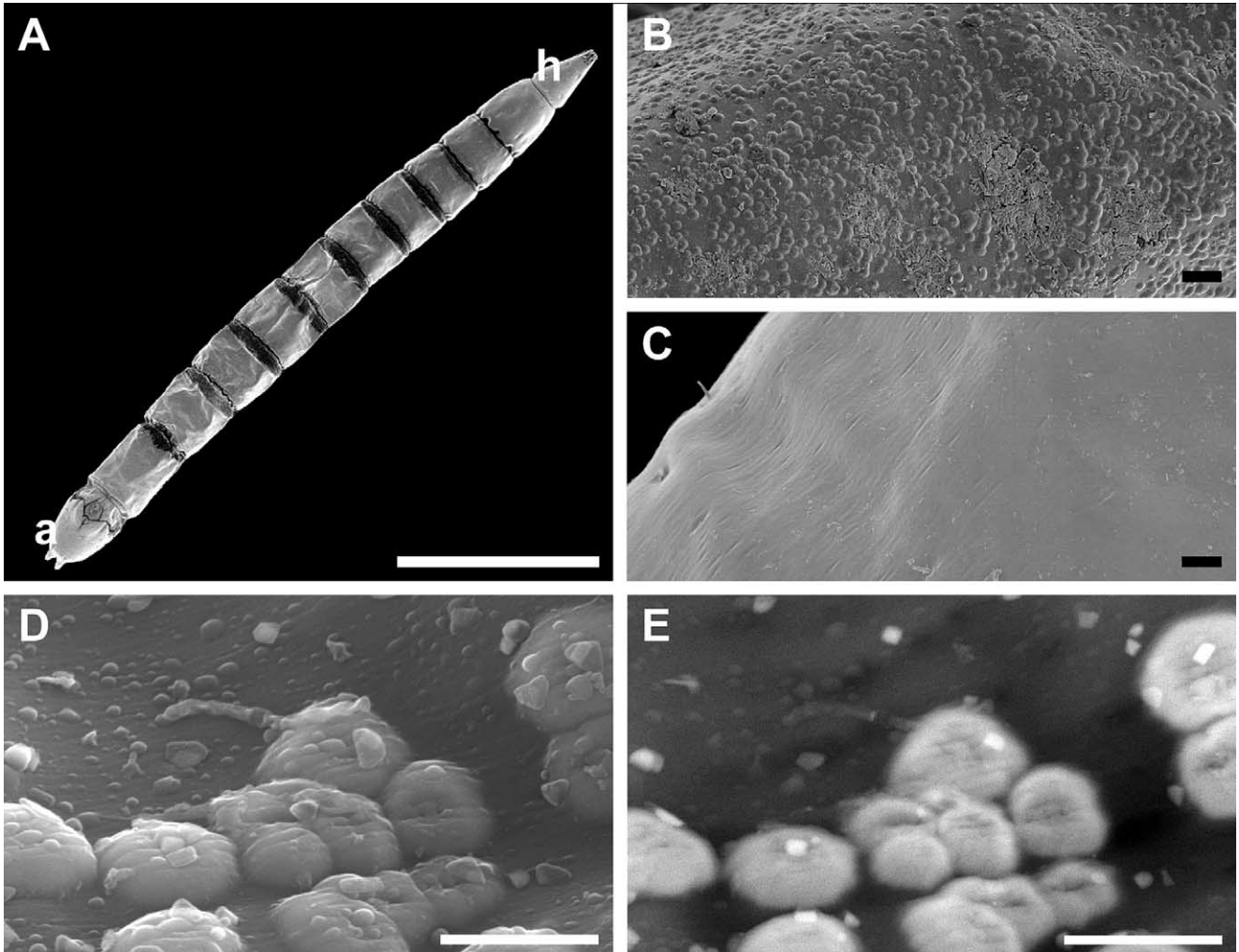


Fig. 1. Scanning electron micrographs of the cuticle of first instar *Exeretonevra angustifrons* showing secondary (SE) and back scattered (BE) electron images. A, An SE image of the whole larva showing pointed head capsule (h) elongate body and anal plate (a); scale bar=1 mm. B, SE image of the body cuticle demonstrating the rough surface; scale bar=10 μm . C, SE image of the head capsule showing a smooth surface; scale bar=10 μm . D, SE image of the hemispheres or domes forming the rough surface on the body; scale bar=5 μm . (E) BE image of the hemispheres and surrounding cuticle seen in D, demonstrating compositional differences through contrast (lighter areas indicate higher atomic number); scale bar=5 μm .

are a maximum of 10 nm in diameter but mostly of 3–7 nm. Results from energy dispersive spectroscopy (EDS) of the cuticle and surrounding resin are shown in Fig. 5. The electron-dense granules show phosphorus (P) and calcium (Ca) peaks, as well as copper peaks, which are associated with the copper grid holding the sections (Fig. 5A). The electron-lucent region within the hemispheres shows much smaller P and Ca peaks (obvious relative to the copper peak) (Fig. 5B) and spot and area analysis of the general cuticle underlying the layer of hemispheres and electron-dense granules shows carbon, nitrogen, oxygen, chlorine, sulphur and P but no Ca (Fig. 5C). Resin adjacent to the cuticle is devoid of P and Ca peaks (Fig. 5D).

The amorphous nature of the mineral phase was confirmed by comparing the $K\alpha$ peak areas of the calcium and phosphorus from the insect cuticle sample with pulverised Durango-apatite (fluoro-apatite standard). Electron diffraction patterns (Fig. 6) and an absence of crystal

lattice (as seen for thin films of ACP: Brès et al., 1993) also confirmed that the granules contained ACP.

3.4. Electron microprobe analysis

Under microprobe analysis colour-coded maps were generated for nitrogen (N), sulphur (S), Ca and P distribution (Fig. 7). In the body region, Ca and P were coincident and mapping showed them in the cuticle. These did not overlap with the bulk of S, which occurred within the body tissue beneath the cuticle. N overlapped in occurrence with Ca, P and S.

4. Discussion

This study investigates the nanostructure and hierarchical distribution of calcium in a Dipteran species.

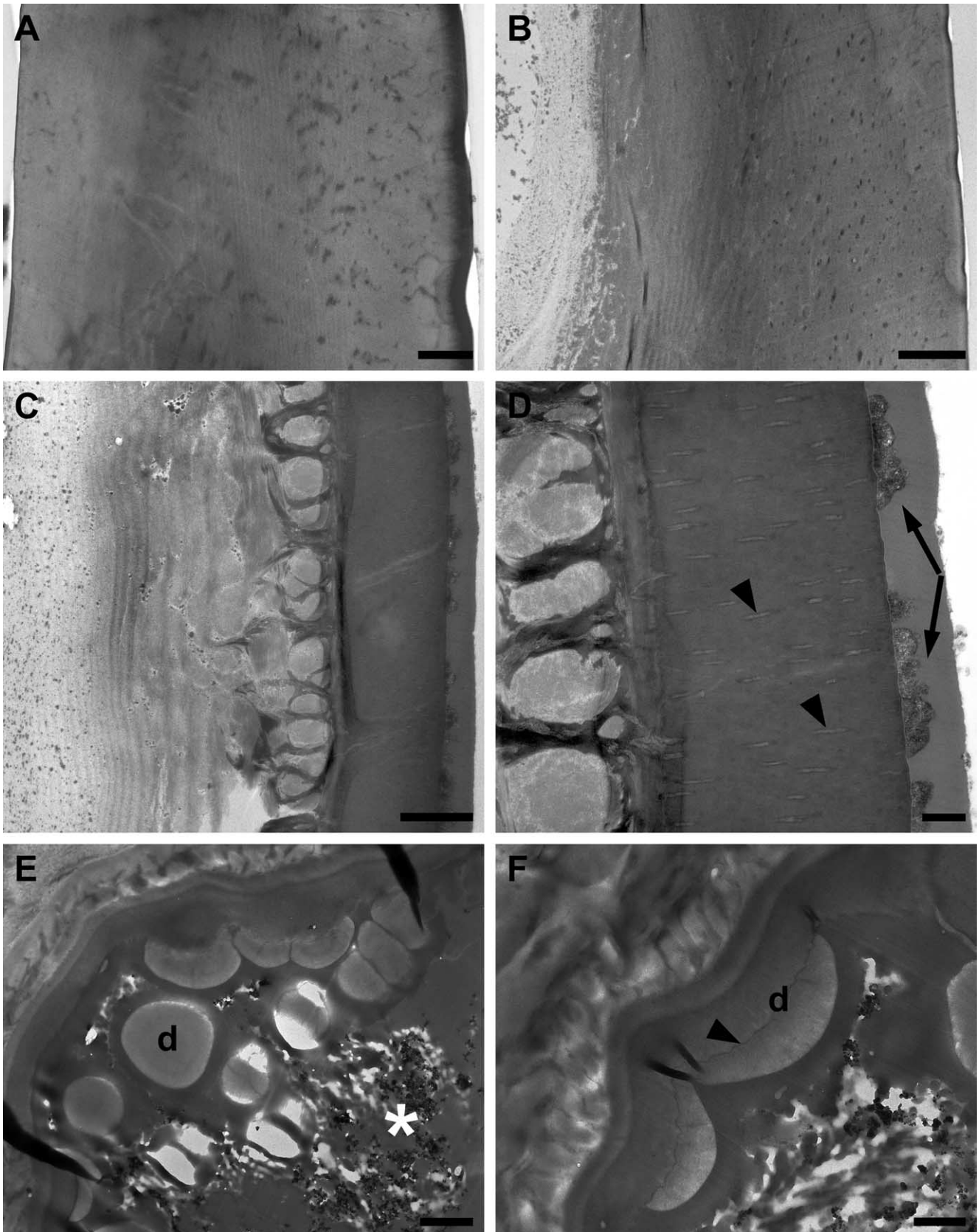


Fig. 2. Transmission electron micrographs of cuticle from *Exeretonevra angustifrons*, contrasted with lead citrate and uranyl acetate, with external surface to the right. A, Head capsule; scale bar = 1 μm. B, Anal plate; scale bar = 2 μm. C, Body cuticle; scale bar = 2 μm. D, Epicuticle of body showing concretions in outer epicuticle (arrows): Note pore canals in inner epicuticle (arrowheads); scale bar = 500 nm. E, Waxes/cement (asterisk) overlying epicuticular

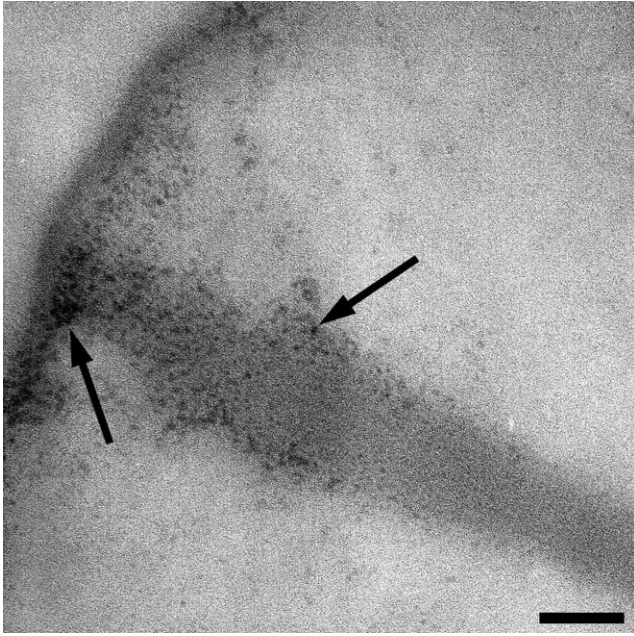


Fig. 3. Unstained transverse section through the body cuticle from *Exeretonevra angustifrons* observed in negative contrast with transmission electron microscopy. Dark granules (arrows) indicate particles of amorphous calcium phosphate; scale bar=100 nm.

Biom mineralisation using calcium is common to a number of invertebrate groups but is rare in the insects, principally having been found in puparia of higher flies (Fraenkel and Hsiao, 1967; Gilby and McKellar, 1976; Grodowitz and Broce, 1983; Roseland et al., 1985; Grodowitz et al., 1987). In contrast we have investigated calcium accumulation in larval cuticle of the xylophagid, *Exeretonevra angustifrons*. This taxon is considered to have an ancient lineage. Because of its limited distribution and specialised biology the species is likely to have existed on the Australian continent for the last 200 million years (Palmer and Yeates, 2000).

Initial analysis demonstrated that head, body and anal plate differed in morphology and composition of the cuticle. Microprobe analysis allowed mapping of elements across the body of first instar larvae to be studied on a broad scale. This demonstrated variation in distribution, with the elements Ca and P coincident in the body cuticle. It showed that nitrogen (indicative of proteins) extends into the calcium bearing tissues yet the sulphur signal falls away in the calcium bearing tissue, possibly indicating that one form of tissue hardening gives way to another. Observations using SEM and TEM showed that the epicuticle was multilayered with hemispherical shaped protrusions at the surface. Within these hemispheres and in a band directly below them, AEM/EDS measured calcium phosphate laid down in an amorphous form, principally present as nanoclusters.

In the higher Diptera, puparial cuticle is mechanically

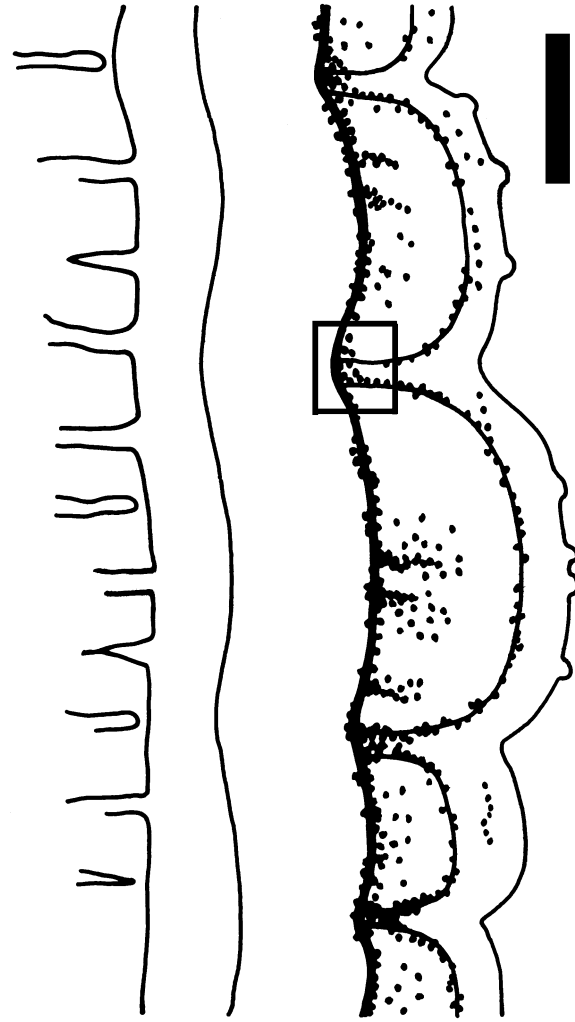


Fig. 4. Diagram of epicuticle from *Exeretonevra angustifrons* showing layers and granules of ACP: box indicates area in Fig. 3; scale bar=2 μ m.

strengthened in two different ways: via sclerotisation and mineralisation, the latter involving Ca, Mg and P (Grodowitz et al., 1987). *Musca autumnalis* uses calcium phosphate and this produces a stiffer, thicker puparial wall (Grodowitz and Broce, 1983; Grodowitz et al., 1987), however little is known about the ultrastructure of biom mineralisation or the mineral form involved. Also, other studies have shown that calcium is absent in larval and adult cuticles of some species, even when it is present in the puparium (e.g. *Musca fergusonii*: Gilby and McKellar, 1976).

Unlike the Insecta, a considerable amount is known about calcium use in the cuticle of Crustacea (Horst and Freeman, 1993). This cuticle has a number of similar characteristics to that of insects so comparisons may be useful. Whereas crystalline calcium carbonate is considered to be the principal structural component of crustacean cuticle with its regulation understood (Burgess and

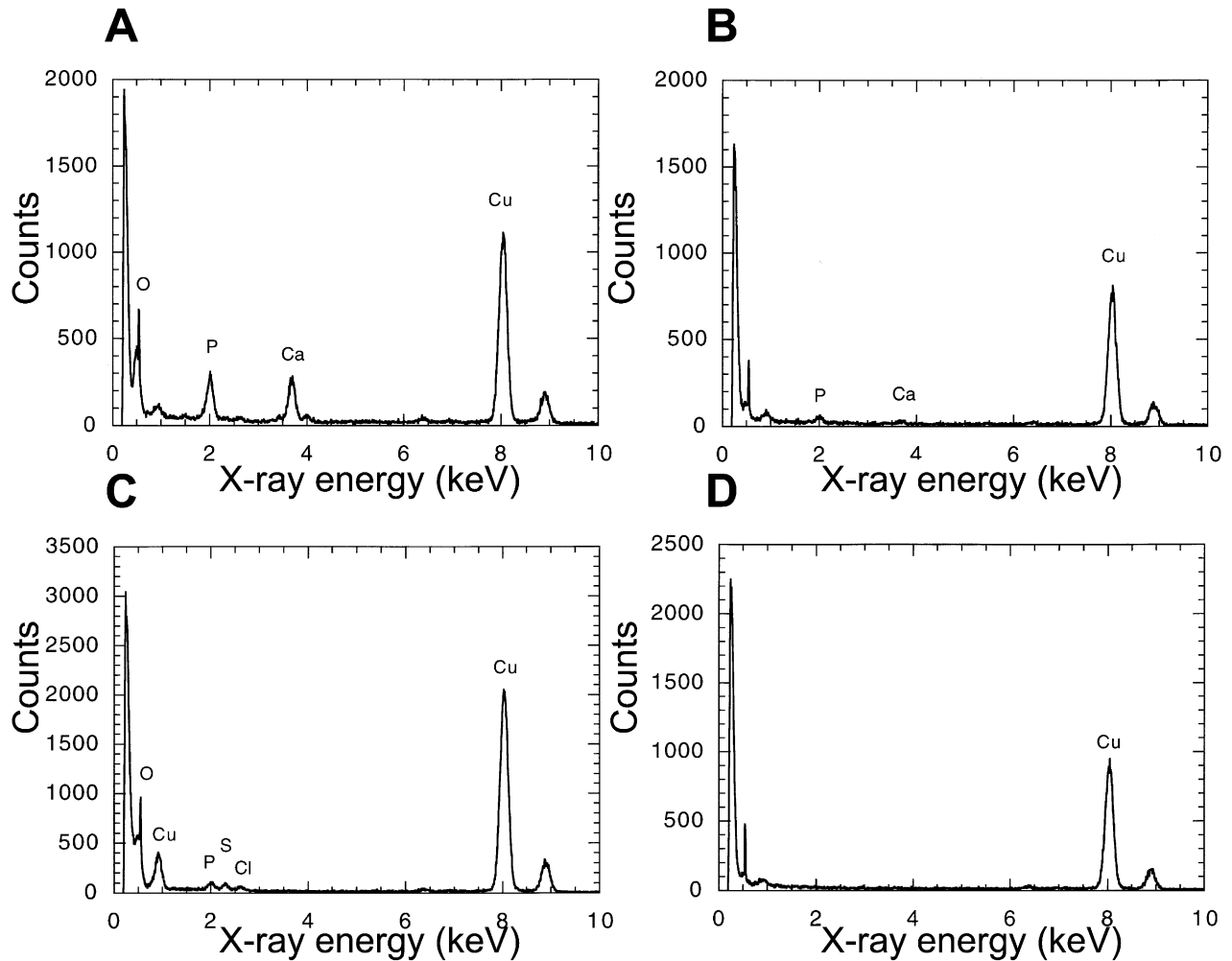


Fig. 5. Energy dispersive spectroscopy of the cuticle of *Exeretonevra angustifrons*. Peaks indicating copper (Cu) can be attributed to the copper mounting grids. Unlabelled peaks left of the oxygen (O) peak represent carbon and nitrogen. A, Spot analysis of electron-dense granules (see Figs. 3 and 4). B, Spectrum from region containing hemispheres but excluding obvious electron-dense granules. C, Spectrum from cuticle below electron dense line at base of hemispheres. D, Spectrum from resin surrounding tissue.

Oxendine, 1995), both calcium carbonate and calcium phosphate are also considered to be associated with hardening of the cuticle and in stomatopods, which are well known for their hard cuticle, a greater concentration of

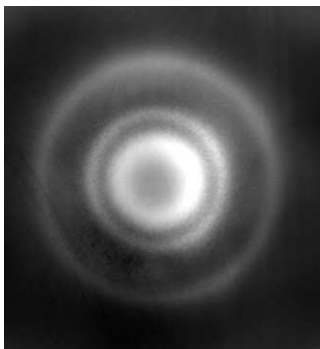


Fig. 6. Electron diffraction pattern from an electron-dense granule (as seen in Fig. 3) with diffraction rings demonstrating amorphous nature of the calcium phosphate material.

calcium phosphate is present in the hardest, outer layer (Currey et al., 1982). Does ACP play a similar role in *Exeretonevra angustifrons*; strengthening the outer layer?

Direct measurement of hardness in such a heterogeneous edge, using classical measures like nanoindentation (see Oliver and Pharr, 1992) does not provide meaningful data so other factors must be considered. Incorporation of ACP is either the result of storage, or fabrication of a cuticle with physical properties suitable for larval life. Since ACP is present in the first instar larva, storage is unlikely to be the explanation. However investigation of other instars might test the theory. Instead, it is more likely that the presence of ACP is associated with improving durability or hardness of the cuticle. Unlike other body regions, sections through regions with numerous hemispheres suffered tears and multiple knife marks during sectioning, indicating particularly hard material. As *Exeretonevra angustifrons* larvae are soil-dwelling (see Palmer and Yeates, 2000), the surface would be subject to considerable abrasion. Possibly the

micron-sized domes, rich in ACP, provide hardness and durability while the surrounding cuticle ensures flexibility. Grodowitz et al. (1987) noted a lack of flexibility in the thick calcified puparial cases of *M. autumnalis* when compared with sclerotized puparia of another species.

More evidence in support of the use of ACP for modification of physical properties comes from ultrastructure. The body epicuticle of *Exeretonevra angustifrons* is penetrated by numerous pore canals, which appear absent from head and anal plates. Presence of such pore canals has been found to be characteristic of arthropod (including insect) cuticle that undergoes biomineralisation associated with increased hardness utilising such elements as Zn, Mn and Fe (Schofield et al., 2003). In the crab *Carcinus maenas*, these pore canals have been found to be the delivery system for calcium and associated minerals prior to crystallisation (Compère et al., 1993).

Understanding the microstructure of biomineralisation in cuticle and associated physical properties provides a source of data for novel materials fabrication. Incorporation of data from cuticle studied on a similar scale for fibre orientation has already led to improvements in the manufacturing of polymers with reduced crack generation and propagation around holes (Vincent, 2003).

References

- Brès, E.F., Moebus, G., Kleebe, H.-J., Pourroy, G., Werkmann, J., Ehret, G., 1993. High resolution electron microscopy study of amorphous calcium phosphate. *Journal of Crystal Growth* 129, 149–162.
- Burgess, S.K., Oxendine, S.L., 1995. A comparison of calcium binding in *Callinectes sapidus* premolt and postmolt cuticle homogenates: Implications for biomineralization. *Journal of Protein Chemistry* 14, 655–664.
- Compère, P., Morgan, J.A., Goffinet, G., 1993. Ultrastructural location of calcium and magnesium during mineralisation of the cuticle of the shore crab, as determined by the K-pyroantimonate method and X-ray microanalysis. *Cell and Tissue Research* 274, 567–577.
- Currey, J.D., Nash, A., Bonfield, A.N.W., 1982. Calcified cuticle in the stomatopod smashing limb. *Journal of Materials Science* 17, 1939–1944.
- Fraenkel, G., Hsiao, C., 1967. Calcification, tanning and the role of ecdyson in the formation of the puparium of the facefly, (*Musca autumnalis*). *Journal of Insect Physiology* 13, 1387–1394.
- Gilby, A.R., McKellar, J.W., 1976. The calcified puparium of a fly. *Journal of Insect Physiology* 22, 1465–1468.
- Grodowitz, M.J., Broce, A.B., 1983. Calcium storage in face fly (Diptera: Muscidae) larvae for puparium formation. *Annals of the Entomological Society of America* 76, 418–424.
- Grodowitz, M.J., Roseland, C.R., Hu, K.K., Broce, A.B., Kramer, J.K., 1987. Mechanical properties of mineralized and sclerotized puparial cuticles of the flies *Musca autumnalis* and *M. domestica*. *The Journal of Experimental Zoology* 243, 201–210.
- Horst, M.N., Freeman, J.A., 1993. *The Crustacean Integument*. CRC Press, Boca Raton, FL.
- Oliver, W.C., Pharr, G.M., 1992. An improved technique for determining hardness and elastic modulus using load and displacement sensing indentation experiments. *Journal of Materials Research* 7, 1564–1583.
- Palmer, C.M., Yeates, D.K., 2000. Phylogenetic importance of immature stages: solving the riddle of *Exeretonevra* Macquart (Diptera: Xylophagidae). *Annals of the Entomological Society of America* 93, 15–27.
- Rasch, R., Cribb, B.W., Barry, J., Palmer, C.M., 2003. Application of quantitative analytical electron microscopy to the mineral content of insect cuticle. *Microscopy and Microanalysis* 9, 1–3.
- Roseland, C.R., Grodowitz, M.J., Kramer, K.J., Hopkins, T.L., Broce, A.B., 1985. Stabilization of mineralized and sclerotized puparial cuticle of muscid flies. *Insect Biochemistry* 15, 521–528.
- Schofield, R.M.S., Nesson, M.H., Richardson, K.A., Wyeth, P., 2003. Zinc is incorporated into cuticular ‘tools’ after ecdysis: the time course of the zinc distribution in ‘tools’ and whole bodies of an ant and a scorpion. *Journal of Insect Physiology* 49, 31–44.
- Vincent, J.F.V., 2003. Biomimetic modelling. *Philosophical Transaction of the Royal Society of London Series B* 358, 1597–1603.

Fig. 7. Elemental map of a first instar *Exeretonevra angustifrons* through a longitudinal section of the body (excluding head and anal plate). Note: anterior region (ant) tangential. Images show distribution of Ca, P, S and N: colour change on vertical axis in legend indicates concentration (white is highest, blue lowest). A monochrome scanning electron micrograph of a similar but enlarged region shows the rough surface of the cuticle; scale bar=20 µm.